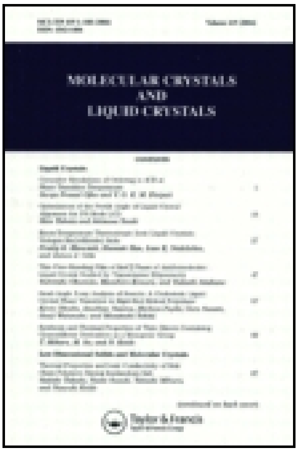

Molecular Crystals and Liquid Crystals Science and Technology. Section A. Molecular Crystals and Liquid Crystals
Publication details, including instructions for authors and subscription information:
http://www.tandfonline.com/loi/gmcl19

# Structural Characteristics of Smectic Liquid Crystals in Main-Chain Polyesters

Junji Watanabe [a] , Manabu Hayashi [a] , Atsushi Morita [a] & Teruki Niiori [a]
[a] Department of Polymer Chemistry, Tokyo Institute of Technology Ookayama, Meguro-ku, Tokyo, 152, Japan

To cite this article: Junji Watanabe , Manabu Hayashi , Atsushi Morita & Teruki Niiori (1994): Structural Characteristics of Smectic Liquid Crystals in Main-Chain Polyesters, Molecular Crystals and Liquid Crystals Science and Technology. Section A. Molecular Crystals and Liquid Crystals, 254:1, 221-240

To link to this article: http://dx.doi.org/10.1080/10587259408036078

*Mol. Cryst. Liq. Cryst.* 1994, Vol. 254, pp. 221–240
Reprints available directly from the publisher
Photocopying permitted by license only

Printed in the United States of America

# STRUCTURAL CHARACTERISTICS OF SMECTIC LIQUID CRYSTALS IN MAIN-CHAIN POLYESTERS

JUNJI WATANABE, MANABU HAYASHI, ATSUSHI MORITA AND TERUKI NIIORI
Department of Polymer Chemistry, Tokyo Institute of Technology,
Ookayama, Meguro-ku, Tokyo 152, Japan

*(Received: February 7, 1994)*

Abstract: Structural characteristics of smectic liquid crystals observed in main-chain BB polyesters are presented.

In the main-chain liquid crystalline polymers, the mesogenic groups within a polymer backbone are linked to each other through a flexible spacer. Each mesogenic group participates to form the mesophase structure as in the low-molecular-weigth material, but in this case. the polymer molecule must adopt a conformation or packing that is compatible with the structure of the mesophase. As a result, the mesogenic properties are closely coupled with the polymeric properties. Considering that the polymer conformation is dominated by the conformation of flexible spacer, an alteration of the flexible group may influence the molecular packing into a mesophase and result in the properties which depart from those of the low-molecular-weight mesogen.

In this paper, forcusing on this coupling effect, we will review our experimental data on the structural characteristics of smectic liquid crystals which have been collected through the studies on the main-chain liquid crystalline BB polyesters with the bibenzoate group as a common mesogen,[1-9]

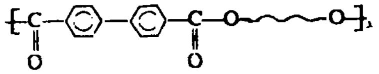

First, we will describe the smectic structural characteristics clarified through the odd-even effect in which the smectic layer structure appears different depending on the odd-even parity of methylene unit in a flexible spacer. We will secondly present how the introduction of branched spacer affects the molecular packing into a smectic layer. By keeping these effects in mind, we will thirdly show that the two types of chiral smectic C liquid crystals with the ferroelectric and antiferroelectric properties can be built up.

## 1. Coupling Effects of Polymeric and Mesogenic Properties

### 1-1. Odd-Even Effects on Smectic Properties and Structures

At first we refer to the BB-n polyesters with the linear alkylene spacers having the carbon number of n.

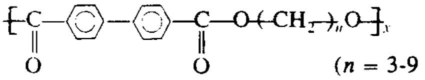

**BB-*n***

($n$ = 3-9 : the carbon number of alkylene group ).

These BB-n polyesters with n of 3 to 9 exhibit two transitions in DSC thermograms.[1,2] Thermodynamic data of BB-n polyesters based on DSC are given in Figures 1a and 1b. Figure 1a shows the variation of the transition temperatures with n. Here, one can find a simple trend that the mesophase temperature region decreases with the increase of n and finally the mesophase disappears when n exceeds 10. The istropization entropies of liquid crystals are given in Figure 1b. Both Figures

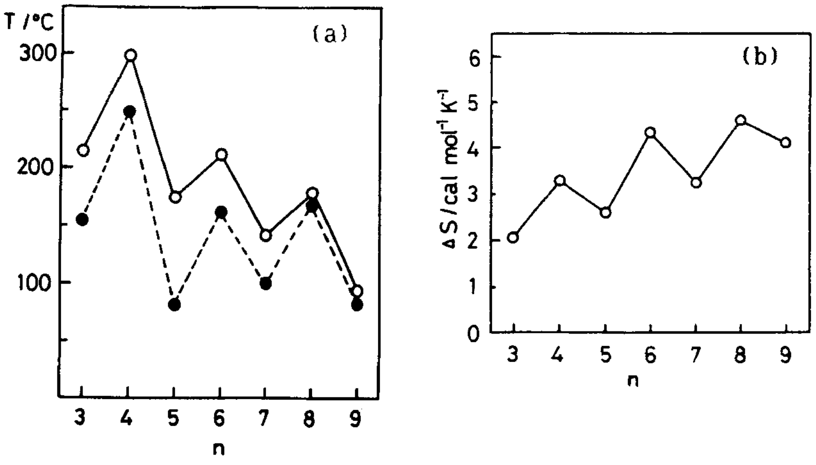

Figure 1. Variation of (a) transition temperatures (●, for the crystal to liquid crystal transition; o, for isotropization of liquid crystal) and (b) isotropization entropy of liquid crystal, with the carbon number of alkylene spacer, n.

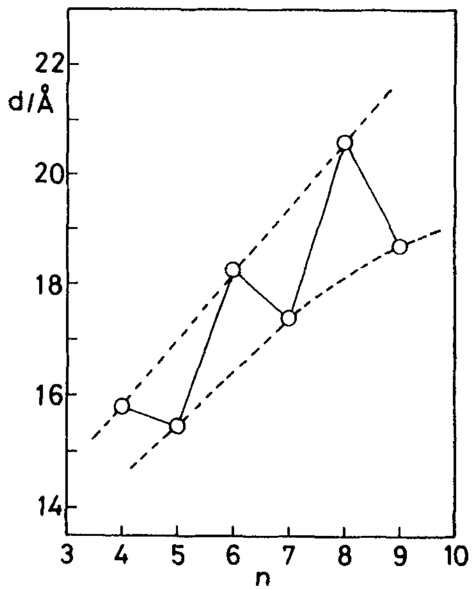

Figure 2. Variation of the layer thickness with n.

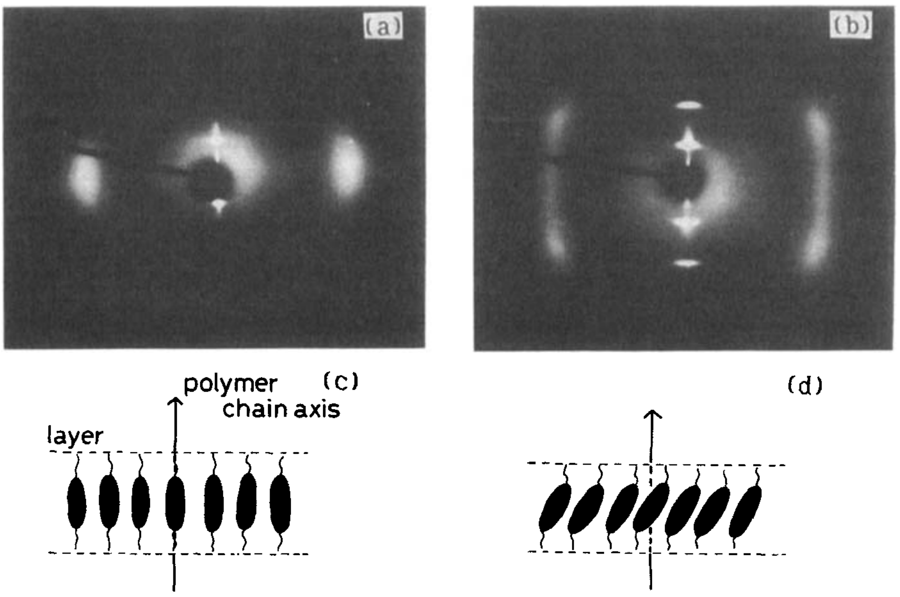

Figure 3. Oriented x-ray patterns taken for the fibrous smectic phases of (a) BB-6 and (b) BB-5. The packing structures of mesogenic groups within a layer elucidated from the x-ray patterns are also illustrated in (c) and (d). Here, the oriented fibers were prepared by pulling the isotropic melt and the fiber axis is placed in the vertical direction.

indicate the clear odd-even oscillation in which the larger values are observed in even membered BB-n polyesters.

The mesophases observed here can be assigned to the smectic phase from the x-ray observations of the sharp inner layer reflection and the outer broad reflection and also from the microscopic observation of the fan-shape texture. The spacing of the inner reflection, i.e., the smectic layer thickness, are plotted against n in Figure 2. Also here, the odd-even oscillation can be seen with a larger spacing for the even membered BB-n polyesters.

The most striking feature in this system is that the smectic structure appears different depending on the odd-even parity of n. This has been initially detected from the x-ray diffractions examined for the oriented fiber specimens.[3] Figures 3a and 3b show the x-ray diffraction patterns of the oriented smectic phases of BB-6 and BB-5, representative materials of even and odd membered polymers, respectively. In BB-6, as found in Figure 3a, the layer reflections appear just on a meridional line and the broad reflections are located on an equatorial line. This diffraction geometry unambiguously indicates the smectic A structure in which the mesogenic groups forming a layer are arranged parallel to the polymer chain and both are perpendicular to the layers (see Figures 3c and 4a).

The BB-5 polyester, on the other hand, shows the distinct x-ray pattern; the broad reflections are split into two portions lying above and below the equator while the layer reflections arise on a meridional line as in BB-6 (see Figure 3b). In this case, hence, the layered

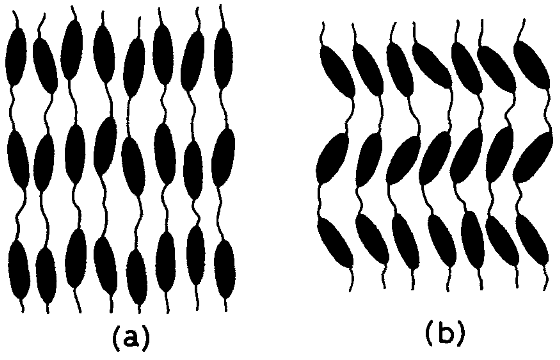

Figure 4. Layer structures of (a) BB-6 and (b) BB-5 smectic phases.

packing structure can be illustrated such that the polymer chains lie perpendicular to the layer as in BB-6 but the mesogenic groups are tilted to the layer normal (see Figure 3d). Tilt angle is independent of temperature and about 25° as can be elucidated from the splitting angle of the broad reflections. The structure is thus similar to the smectic C as far as the arrangement of the mesogenic groups within a layer is concerned.

The smectic structure in odd-membered BB-n can be uniquely determined from the observation of optical texture in homeotropic specimens.[6] The optical microscopic texture of the homeotropic specimen of BB-5 is given in Figure 5. It exhibits the high birefringence and also shows the various schlierens. These observations, together with the x-ray observations, undoubtedly show that the c-director exists in each layer and its orientation correlation is maintained from the layer to layer. To be emphasized here is a fact that the schlieren texture with the singularities of $s = 1/2$ as well as $s = 1$ can be observed. This means that the continuous variation of c-director orientation around the disclination of $s = 1/2$ is promised in this smectic phase, obviously ruling out the assignment to the smectic C.[10] From the

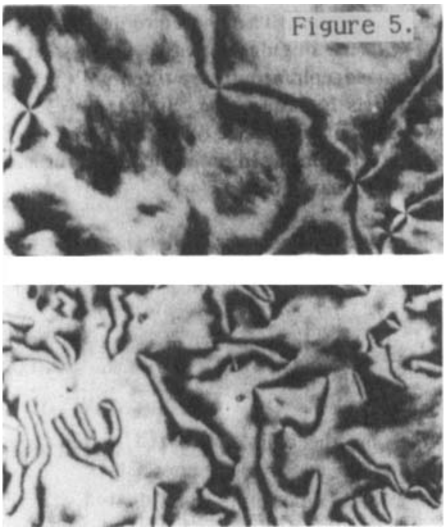

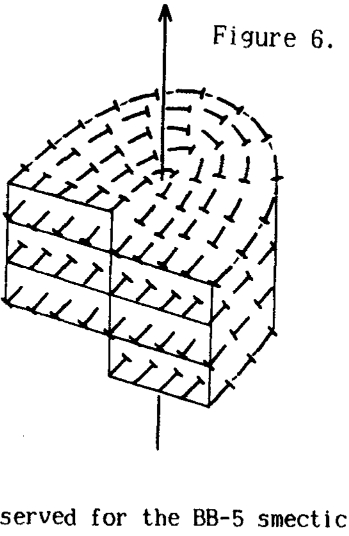

Figure 5. The optical microscopic texture observed for the BB-5 smectic phase in a homeotropic alignment.

Figure 6. The c-director orientation around the wedge dispiration with rotational component of $\pi$ which can be expected for the $S_{C2}$ phase. The translational component gives rise to the step.

detailed examination,[6-8] one can find only a smectic structure, as illustrated in Figure 4b, in which the mesogenic groups are tiled with repect to the layer normal, but unlike the smectic C phase the tilt direction is opposite in adjacent layers.[6] In this smectic phase, the disclination of $s = 1/2$ can be allowed for the c-directors as illustrated in Figure 6. Here, the edge disclination is coupled with the helical dislocation, that is, one layer is shifted to its neighboring layer after the rotation of 180° around the disclination line. This combined deffect with the edge disclination and helical dislocation is called a dispiration.[6,7,11]

As a conclusion, the even-series of BB-n form the $S_A$ in which both axes of polymer chain and mesogenic group lie perpendicular to the layer (Figure 4a), while the odd-membered ones form the disinct smectic phase in which the polymer chains are perpendicular to the layer but the mesogenic groups are tilted to the layer in an alternate fashion (Figure 4b). We call here this distinct phase the $S_{C2}$ to differentiate from the normal $S_C$ phase. In most types of liquid crystals so far observed, uniaxial orientation has been achieved for the long axes of the mesogens. In this sense, the $S_{C2}$ phase observed here is quite novel and interesting since uniaxial ordering cannot be observed for the n-director but only for the c-director.

### 1-2. Polymer Conformation in Smectic Phase.

The odd-even appearance of smectic layered structure and the formation of the curious and novel $S_{C2}$ structure are believed to result from a coupling effect of the polymeric and mesogenic properties in which the spatial arrangement of mesogenic groups is strongly related to the conformation of the intervening alkylene spacers.

In order to account for this effect, Abe[12] has performed conformational analysis of the flexible spacer, within a framework of the rotational isomeric state model, and evaluated the angle $\theta$, defined by unit vectors attached to two successive mesogenic groups.

The results are shown in Figure 7 where the relative numbers of conformers are plotted against $\theta$ for BB-6 and BB-5. From this Figure, we can understand that the angular distributions appear different between the even- and odd-series of BB-n polymers. When n is even, $\theta$ are found to be distributed in the two ranges 0 to 20° and 90 to 120°.

For n is odd, the major portion of the angles is located in the region 50 to 90° and to some degree orientations are also permitted in the region above 150°. In each system, the conformers with the smaller angular displacement of successive mesogens are in the more extended form whereas the conformers with the larger angular displacement are in the folded form. According to this calculation, we can arrive at the following conculsions which are closely related to the smectic layered structures above observed.

(1) In the n = even series, the parallel orientation of successive mesogenic groups is allowed, conforming more or less to the concept of an ordinary uniaxial ordering of the n-director but in the n = odd series uniaxial orientation of successive mesogenic groups is not expected.

(2) The conformers with the smaller angular displacement in both odd and even systems correspond to the conformers participating in the observed layer structure.

These explain the odd-even appearance in the type of smectic phases and at the same time, account for the specific formation of a $S_{C2}$ phase in the odd-series of BB-n, leading to the reasonable conclusion that the smectic structure is strongly affected by the conformational constraint of a flexible spacer.

This conclusion can be supported by the observation that the averaged spacing between adjacent mesogens calculated for the confined conformers corresponds to the observed layer thickness. This can be seen in Figure 8, where the observed layer thickness is compared to the calculated spacing between the mesogens. One can find that the absolute

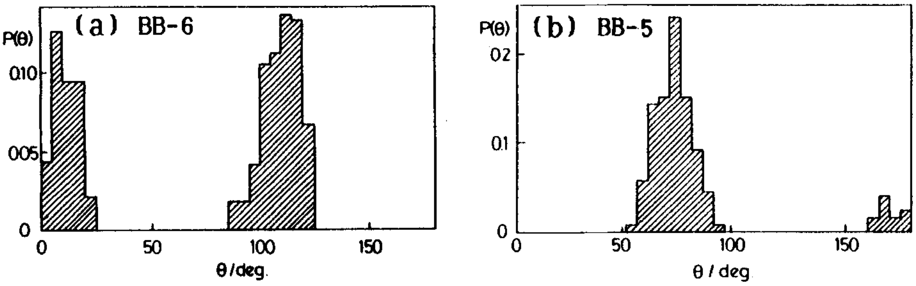

Figure 7. Distribution of chain conformer calculated for the angle θ defined by two successive mesogens; (a) BB-6 and (b) BB-5. The rotational angles and statistical weights in Table II of reference 12 are adopted for the calculation.

values as well as the odd-even oscillation can be perfectly reproduced.

Furthermore, the significance of the conformational constraint can be supported by the fact that dimeric model compounds with the following formula,

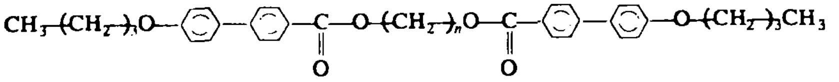

exhibit the same mesomorphic behavior as the BB-n polyesters; the $S_{C2}$ phase is observed if the number of methylene unit in a flexible spacer is odd while the even-membered compounds with n = 4, 6 and 8 show the $S_A$ phase.[9]

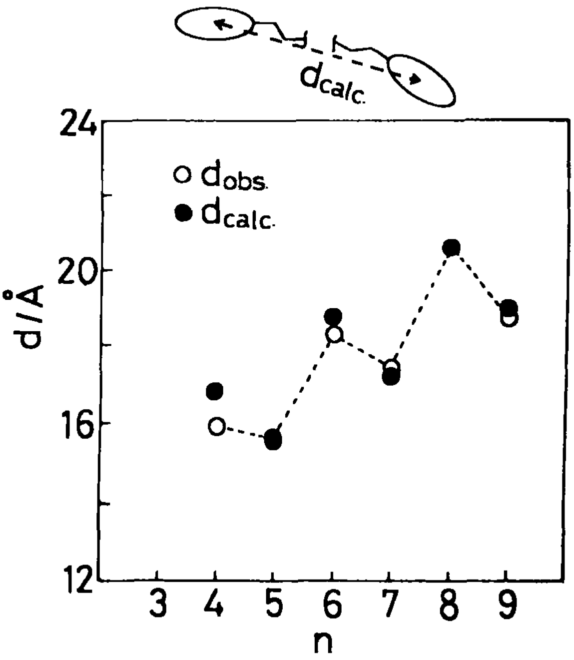

Figure 8. The comparison of the observed layer thickness with the calculated layer thickness which corresponds to the distance between the mesogenic groups averaged over the conformers with the small angular displacement of successive mesogens (refer to Figure 7).

## 2. Effect of Branched Spacer on Smectic Properties and Structure

To clarify this effect, the simple and systematic series of polymers have been prepared by introducing the branched methyl group into the flexible spacer of BB-4.[5] The examples of the polyesters in this series are given below,

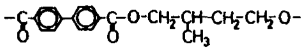
BB-4(2-Me)

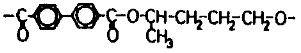
BB-4(1-Me)

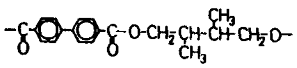
BB-4(2,3-diMe)

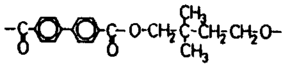
BB-4(2,2-diMe)

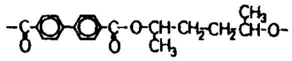
BB-4(1,4-diMe)

and their thermotropic behavior are listed in Table I. Here it is very interesting that the branching of one methyl group alters the smectic A of BB-4 to the smectic C phase, while branching of two methyl groups facilitates the formation of nematic phase. The smectic C layered structure formed by these polyesters is illustrated in Figure 9. Although its detailed description will be given later, the mesogenic groups in this $S_C$ phase are arranged parallel to the polymer chain axis like in the smectic A but both axes are tiled to the layer normal. The tilting of mesogenic groups is considered to result from the steric hindrance between branched groups.

**Table I.** Phase transitions (°C) based on cooling DSC data for the BB-polyesters; $K$=crystal; $S_C$=smectic C; $S_A$=smectic A; $N$=nematic; $I$=isotropic melt; ( )=transition entropies ($\Delta S$) in kcal mol$^{-1}$ of repeat unit K

| | $\eta_{inh}$/dlg$^{-1}$ | Phase transitions | | | | | | | |
|---|---|---|---|---|---|---|---|---|---|
| | | $K$ | | $S_C$ | $S_A$ | | $N$ | | $I$ |
| BB-4 | 0.32 | ● | 251<br>(2.0) | — | ● | | — | 298<br>(3.3) | ● |
| BB-4 (2-Me) | 0.41 | ● | 139<br>(1.4) | ● | — | 185<br>(0.5) | ● | 210<br>(2.9) | ● |
| BB-4 (1-Me) | 0.40 | — | | ● | — | | — | 148<br>(3.7) | ● |
| BB-4 (2,3-diMe) | 0.45 | ● | 127<br>(3.9) | — | — | | ● | 182<br>(2.7) | ● |
| BB-4 (2,2-diMe) | 0.42 | ● | 124<br>(1.8) | — | — | | ● | 162<br>(2.4) | ● |
| BB-4 (1,4-diMe) | 0.35 | — | | — | — | | — | | ● |

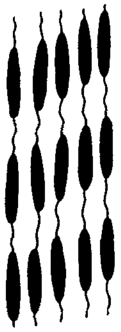

Figure 9. Layer structure of the $S_C$ phase observed in BB-4(2-Me).

## 3. On Ferroelectric and Antiferroelectric Chiral $S_C$ Liquid Crystals

The preceeding studies indicate that the spacer significantly affects the smectic structure and that three types of smectic phases, $S_A$, $S_C$, and $S_{C2}$, can be prepared only by changing the type of spacer. Among these phases, the $S_C$ and $S_{C2}$ are interesting since these can be altered to the chiral ferroelectric and antiferroelectric $S_C$ phases by introducing the chiral flexible spacers. Here, we will describe the mesophase properties of these chiral $S_C$ liquid crystals in polymers.

### 3.1 Ferroelectric Chiral $S_C$ Liquid Crystal

The typical example of the chiral $S_C$ can be observed in BB-4*(2-Me) with the chiral 2-methyl-butylene uint as a flexible spacer,

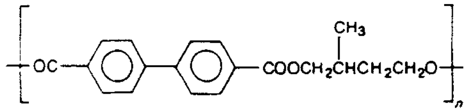

This material exhibits the cholesteric phase in addition to the chiral $S_C$ phase. The chiral $S_C$ phase is monotropic and so appears from 185 to 140$^0$C only on cooling process.

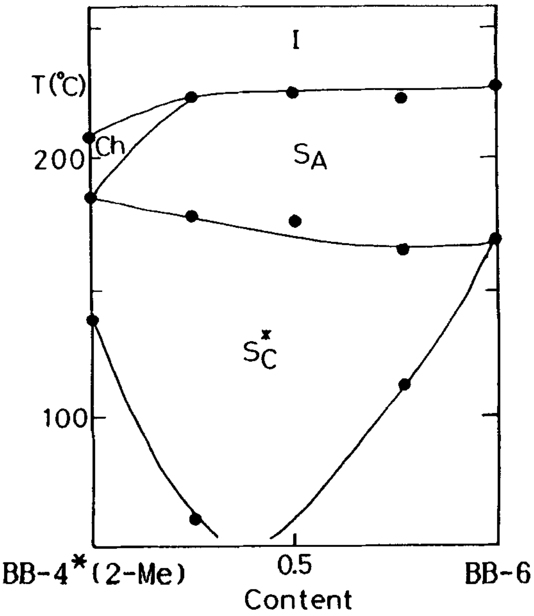

Figure 10. Transition behavior in the copolymers of the chiral BB-4*(2-Me) and BB-6. The transition temperatures were collected from the DSC cooling data.

As more proper specimens giving the enantiotropic chiral $S_C$, the copolymers of BB-4$^*$(2-Me) and BB-6 have been prepared. Figure 10 indicates the transition behavior of copolymers where the transition temperatures are plotted against the BB-4$^*$(2-Me) content. In addition to the cholesteric phase of BB-4$^*$(2-Me) and the $S_A$ phase of BB-6, one can find the enantiotropic chiral $S_C$ phase, which can be attained in the wide temperature region for the copolymers with the intermediate contents as a result of eutectic-like depression of crystal melting.

At first, we try to illustrate the $S_C$ layer structure through the x-ray observations. For this purpose, the copolymer with the equimolar content was used. This copolymer exhibits $S_A$ and $S_C$ phases as found in Figure 10; the transition temperature of $S_A$ to $S_C$ is around 180$^o$C.

Figure 11 indicates the oriented x-ray photographs for the $S_A$ and $S_C$ phases of fibrous specimen. The difference between $S_A$ and $S_C$ is obvious; the meridional layer reflection of $S_A$ becomes split on transition to the $S_C$ while the equatorial reflection still remains on an equator. This indicates that the mesogenic groups are tilted to the layer normal. The tilt angle can be estimated in two methods. At first,

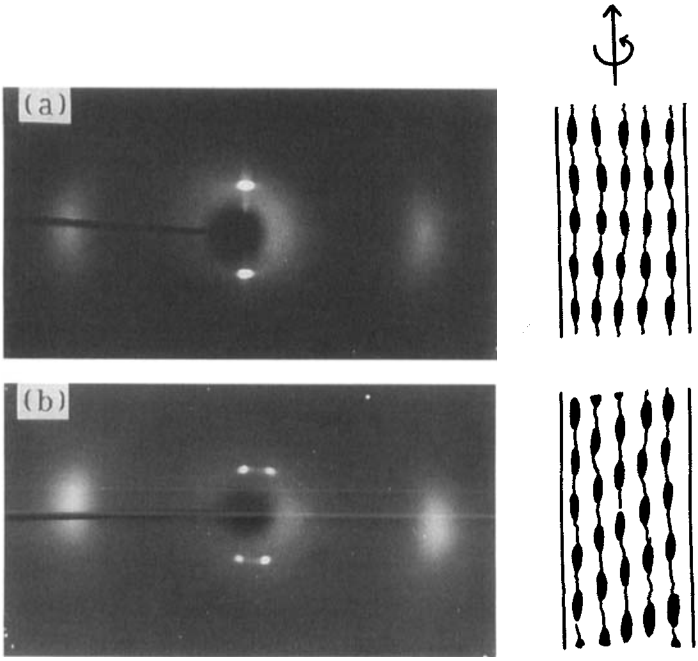

Figure 11. X-ray photographs observed for the oirented smectic phases of equimolar copolymer and the illustration of the layered structures. (a) $S_A$ phase at 200$^o$C; (b) chiral $S_C$ at 150$^o$C.

it can be determined directly by the splitting angle of layer reflection and secondly, indirectly by the reduction of its spacing. Both methods gave the same tilt angle, indicating that the conformation of polymer chain remains unchanged through the mesophase transition from $S_A$ to $S_C$. According to the diffraction geometry, the layered structure in fibrous specimen can be illustrated in Figure 11. Obviously, the tilting of mesogenic groups in $S_C$ have been produced by the staggered packing of polymer chains along a fiber axis such that the polymer chain and mesogenic group are parallel to each other as in $S_A$ but both are tilted to the layer normal. The structure, hence, is similar to the chiral $S_C$ of the low molar materials except that each mesogenic groups are linked to each other. As found in Figure 12, the tilt angle, Θ, increases with the decreasing temperature according to the equation,

$$\Theta \propto (T_C - T)^{0.45}$$

which is also identical to that observed in the low molar $S_C$ phases.

Further evidence of the chiral $S_C$ phase can be given by the observation of helical structure which is produced by the twist of c-directors. Figure 13a indicates the homogeneous texture of chiral $S_C$ observed in the copolymers with the low chiral content of BB-4*(2-Me) unit. The dechiralization lines attributable to the helical twisting can be observed. On the other hand, in the copolymers with the larger

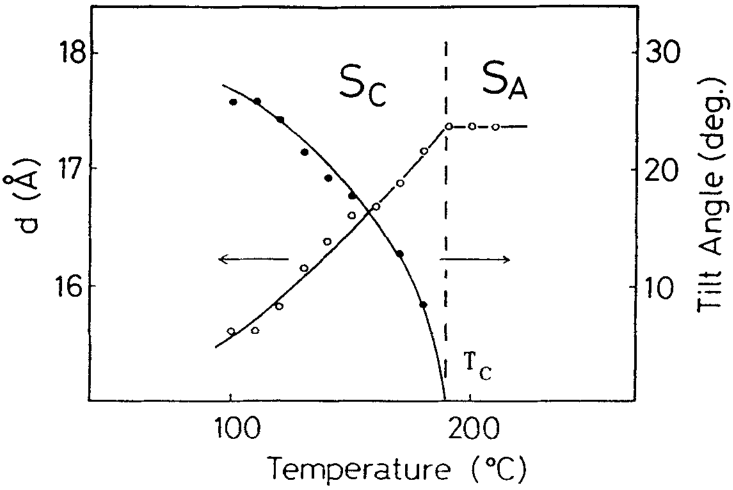

Figure 12. Temperature dependence of the layer thickness and the tilt angle in the smectic phases of equimolar copolymer.

chiral content, the selective reflection of visual light is observed as given in Figure 13b. These indicates the existence of helical structure. For all copolymer specimens, the helical pitch was found less independent of the temperature. In Figure 14, the reciprocal pitches elucidated are plotted against the chiral content of BB-4*(2-Me) unit. Here the closed circles were collected from the microscopic observation and the open circles based on the spectroscopic

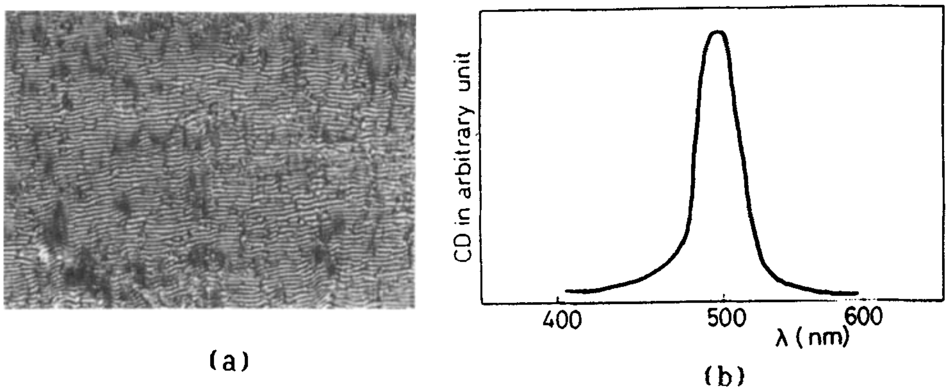

(a)

(b)

Figure 13. (a) Microscopic fan shape texture with the dechiralization lines and (b) the reflection spectra as observed in the chiral $S_C$ phases. See Color Plate II.

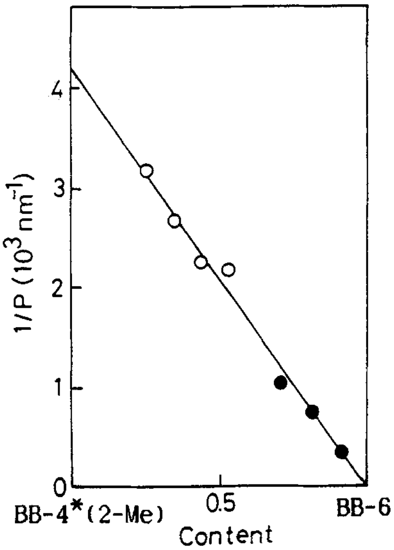

Figure 14. The variation of the reciprocal pitches of the chiral $S_C$ phase with the chiral content of BB-4*(2-Me) unit.

observation of the reflection band. One can find that the reciprocal pitch, that is the twist angle, linearly increases with the increase of chiral content.

Since in the polymeric chiral $S_C$ system the mesogenic groups are linked to each other, the polymer molecule should be also forced to assume a helical conformation. From the structure parameters observed for the chiral $S_C$ of the equimolar copolymer (for example, tilt angle $25^{\circ}$ and layer thickness of 17 A), helical conformation of polymer can be illustrated as having a pitch of 3000 A and a radius of 300 A. The helix is rather loose and so the polymer chain can be approximated to be linear at a local portion, but the bending and twisting deformation in polymer chain is obviously induced.

Although the chiral $S_C$ in polymeric system has thus some different structural characteristic from the low molar mass chiral $S_C$, the polymeric chiral $S_C$ is also ferroelectric. This can be easily recognized from the elimination of helical structrure on applying the high voltage. The spontaneous polarizability, Ps, were determined from the switching current which can be measured by applying triangular wave voltage with a frequency of 1.1 Hz and amplitude of 100 Vp-p. The experimental data of switching current peak is given in Figure 15a. Here, the equimolar copolymer with the relatively low molecular weight

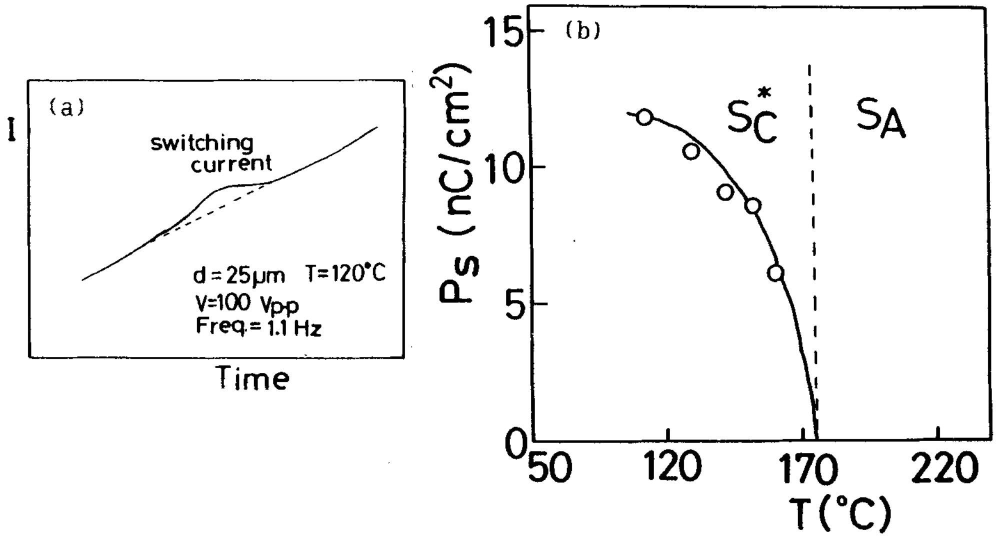

Figure 15. (a) The switching current peak measured by applying the triangular voltage and (b) the temperature dependence of spontaneous polarizability, Ps, observed for the equimolar copolymer (see text).

([$\eta$] = 0.15 dL/g) was used. The values of Ps thus evaluated are plotted against temperature in Figure 15b. There can be seen a similar temperature variation as in the low molar material $S_C$: ferroelectric property arises on the transition from $S_A$ to $S_C$ and the value of Ps increases with decreasing temperature. The maximum value of Ps is around 12 nC/cm$^2$.

### 3.2. Antiferroelectric Chiral $S_{C2}$ Liquid Crystal

The chiral $S_{C2}$ can be observed in the BB-3*(1-Me) polyester with the chiral 1-methyl propylene unit as a flexible spacer as given below.

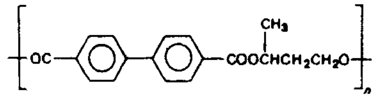

Since the alkylene groups directly linking the mesogenic groups includes three carbons, the polymer satisfies the condition exhibiting the $S_{C2}$ layer structure. In fact, the oriented x-ray pattern for the mesophase of this material has confirmed the $S_{C2}$ structure.

Also here, the copolymers of BB-3*(1-Me) and BB-5 were prepared with the various chiral contents. The phase behavior of copolymers is shown in Figure 16a. Also in this system, it can be found that the

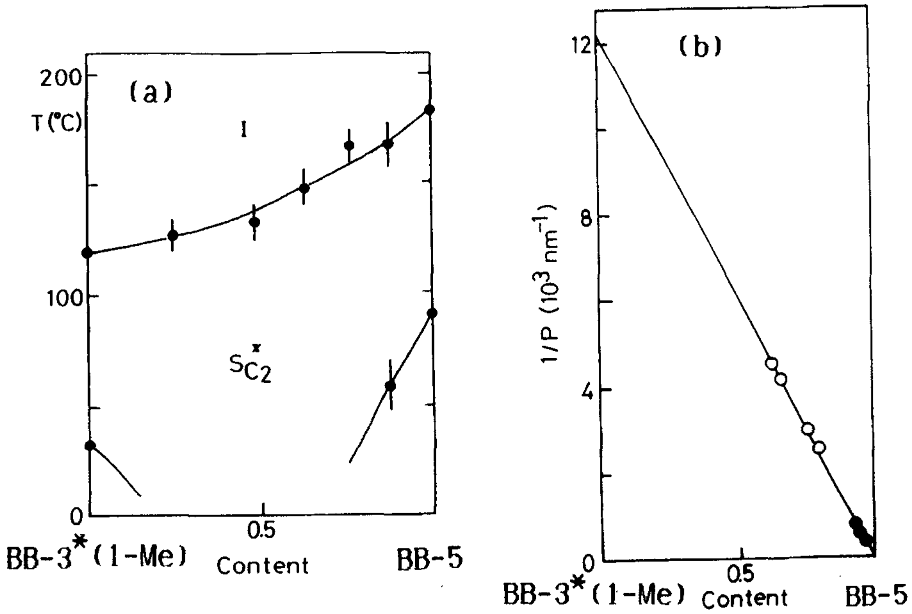

Figure 16. (a) The phase transition behavior in the copolymers of the chiral BB-3*(1-Me) and BB-5 and (b) the variation of the reciprocal pitches of the chiral $S_{C2}$ phase with the chiral content of BB-3*(1-Me).

eutectic-like depression of crystal melting gives the wide temperature region of the chiral $S_{C2}$. The formation of the helical structure has been also confirmed by the optical microscopy and spectroscopy. The variation of the reciprocal pitch with the chiral content of BB-3*(1-Me) unit is shown in Figure 16b.

In this case, the illustration of helical structure is somewhat complicated since the $S_{C2}$ phase has an alternate tilting of mesogenic groups in successive layers and so the two different sets of c-director vectors. By this reason, the resultant helical structure should be essentially different from that of the normal $S_C$ which has only a set of c-director vector, and can be regarded as identical to two chiral $S_C$ helices geared into each other with a phase difference of $\pi$. In Figure 17, such a peculiar helical structure is schematically illustrated and compared with the helical structure of chiral $S_C$.

Such a difference in a helical structure between the chiral $S_{C2}$ and $S_C$ can be confirmed through the selective reflection property of light. On this point, we first try to figure up helical arrangement of the refractive index ellipsoids. In both $S_C$ phases, the index ellipsoid has

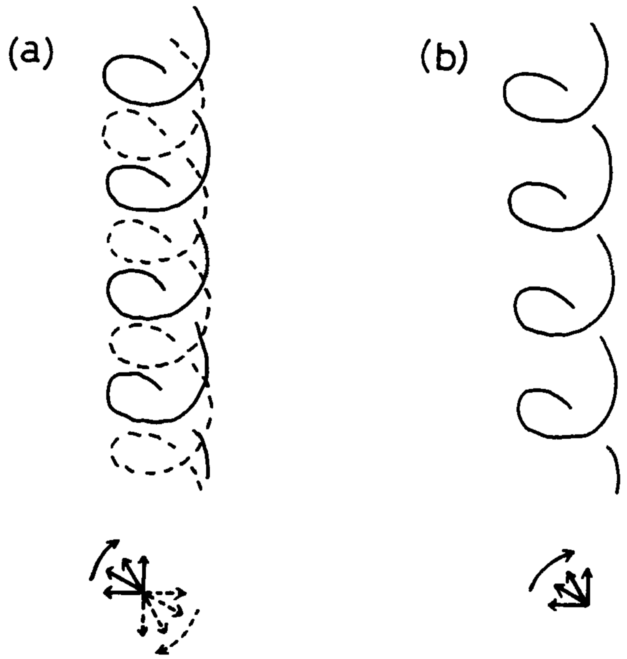

Figure 17. The schematic illustration of the helical arrangement of the c-directors in (a) chiral $S_{C2}$ and (b) chiral $S_C$ phases.

a biaxial nature, as illustrated in Figure 18. In the $S_{C2}$ phase, the unit cell includes two layers and the molecular packing has the crystallographic $D_{2h}$ symmetry.[6,13] Hence, the z-axis giving the maximum

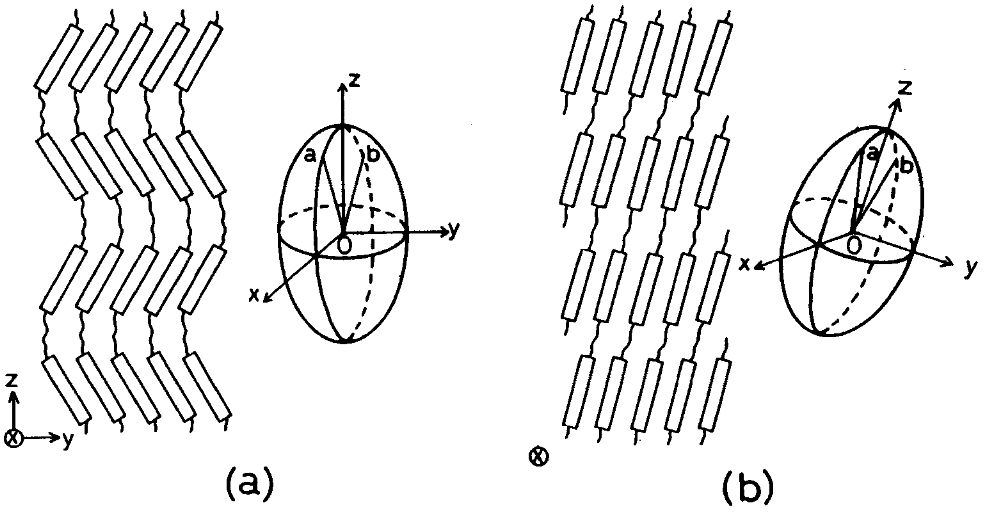

Figure 18. The molecular ordering and its optical index ellipsoid in (a) the $S_{C2}$ and (b) $S_C$ phases.

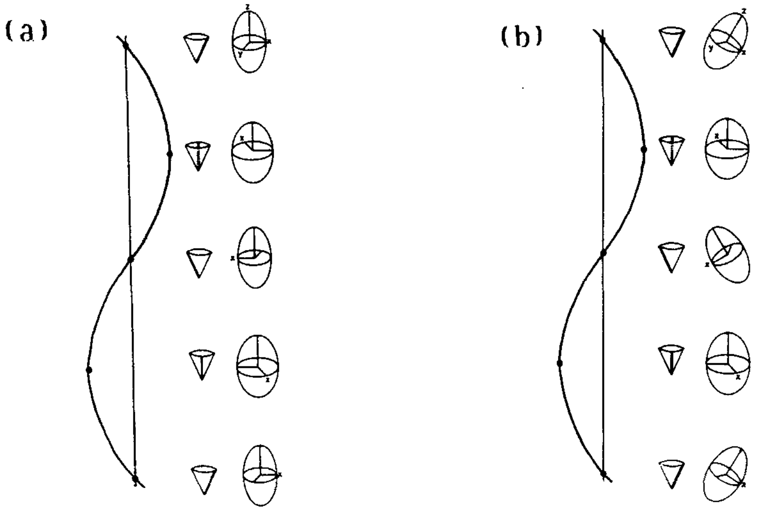

Figure 19. The schematic illustration exhibiting the helical arrangement of the refractive index ellipsoids in (a) the chiral $S_{C2}$ and (b) chiral $S_C$ phases.

refrative index lies perpendicular to the layers as illustrated in Figure 18a. In contrast, in the $S_C$ with the $C_{2h}$ symmetry, the corresponding z-axis is tilted to the layer plane (see Figure 18b).

Since the helical structure is formed along the layer normal, there should arise a remarkable difference in the helical arrangement of the index ellipsoids in both phases. In Figure 19 is illustrated such a different situation. In a helix of chiral $S_C$, the index ellipsoid rotates around the helical axis with a certain tilting of z-axis while in helical chiral $S_{C2}$ it rotates keeping the z-axis parallel to the helical axis. When the light propagates parallel to the helical axis, both phases exhibit the selective reflection of the light with the wavelength equal to a half pitch, since the layer giving the same refractive indices appears in every half pitch. Such a reflection band

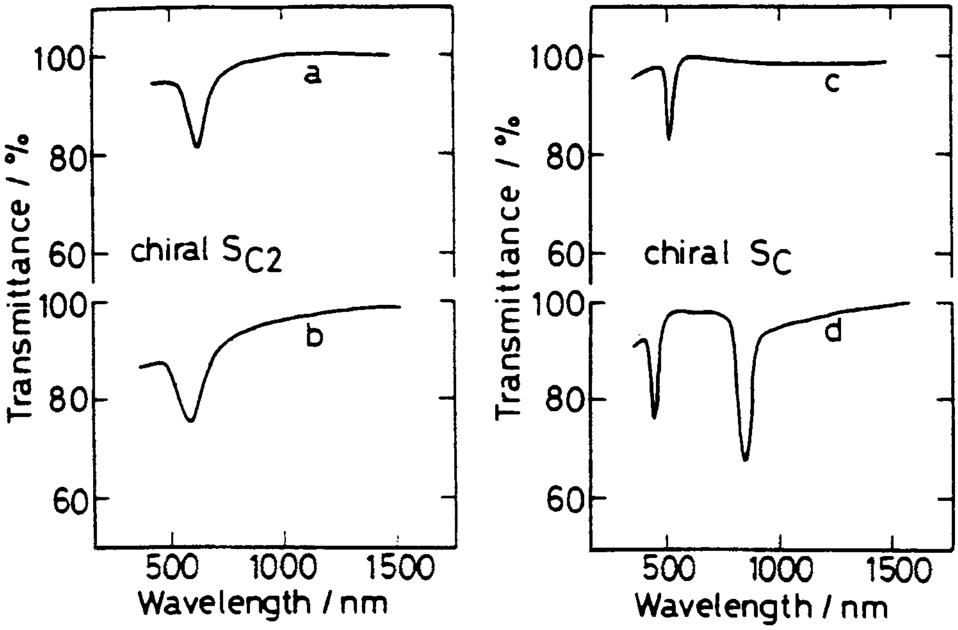

Figure 20. The reflection spectra for chiral $S_{C2}$ and chiral $S_C$ phases with a homeotropic alignment. a) and c) The reflection spectra as measured by the incident light parallel to the helix axis. b) and d) The reflection spectra as measured on incidence inclined by $60^o$ to the helix axis.

is called here a half-pitch band. In contrast, when the light propagates in a tilted direction to the helix axis, the same refractive indices no more appear in every half pitch for the chiral $S_C$ but in every full pitch while in the chiral $S_{C2}$ they still repeat in every half pitch. On tilted irradiation of light to the helix axis, hence, the chiral $S_C$ should newly show a full-pitch band while the chiral $S_{C2}$ should still exhibit only a half-pitch band like a cholesteric phase.[14]

To give the experimental evidence for this, the reflection properties were examined for the homeotropic specimens. The reflection spectra are given in Figure 20. On the irradiation of light parallel to the helix axis, only a half pitch band can be observed for both chiral $S_C$ phases. On the tilted irradiaiton (for example on $60^o$ irradiation), in contrast, the full pitch band appears in chiral $S_C$ but not in chiral $S_{C2}$. The results are thus to be expected, confirming again the structural peculiarity of $S_{C2}$ phase.

Finally, we like to comment on the electric property of $S_{C2}$ phase. In this phase, the molecular packing has locally $C_2$ symmetry in a level of each layer. In this sense, the spontaneous polarizability can be expected to arise as in the chiral $S_C$ (see Figure 21). However, the phase has globally $D_2$ symmetry by coupling of two layers, which entails zero average polarization. Such a phase can be regarded as an antiferroelectric phase.[15-17]

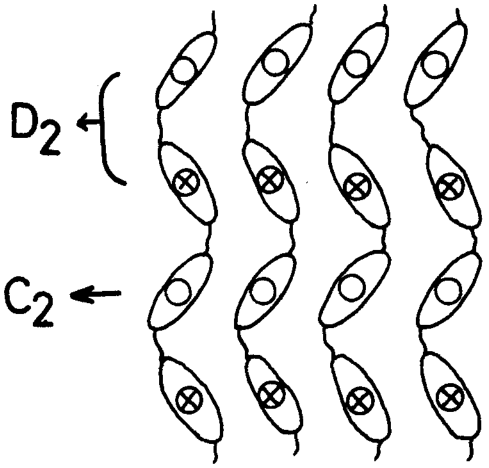

Figure 21. Spontaneous polarization in the chiral $S_{C2}$ phase.

The antiferroelectric properties can be recognized by the observation of the characteristic double D-E hysteresis loop.[17] However, at the present time, such D-E hysteresis loop has not been observed even if the maximum field of 5 KV/mm was applied. Probably, the critical electric field to induce a ferroelectric state may be fairly high, because in this case the induction of ferroelectric property includes the conformational change of polymer in which the resultant conformation may be in an appreciably high energy level.

## REFERENCES

1. W. R. Krigbaum and J. Watanabe, Polymer, 24, 1299(1983).
2. J. Watanabe and M. Hayashi, Macromolecules, 21, 278(1988).
3. J. Watanabe and M. Hayashi, Macromolecules, 22, 4083(1989).
4. H. Takezoe, A. Fukuda, A. Ikeda, Y. Takanishi, T. Uemoto, H. Iwane, M. Hara, K Itoh and J. Watanabe, Ferroelectrics, 122, 167(1991).
5. J. Watanabe, M. Hayashi, S. Kinoshita and T. Niori, Polym. J., 24, 597(1992).
6. J. Watanabe and S. Kinoshita, J. Phys. II (France), 2, 1273(1992).
7. Y. Takanishi, H. Takezoe, A. Fukuda, J. Watanabe and H. Komura, J. Mater. Chem., 2, 71(1992).
8. Y. Takanishi, H. Takezoe, A. Fukuda and J. Watanabe, Phys. Rev. B, 45, 7684(1992).
9. J. Watanabe, H. Komura and T. Niiori, Liquid Crystals, 13, 455(1993).
10. G. W. Gray and J. W. Goodby, Smectic Liquid Crystals, Leonald Hill, Glasgow and London, 1984.
11. W. F. Harris, Philos. Mag., 22, 949(1970).
12. A. Abe, Macromolecules, 17, 2280(1984).
13. A. Michelson, D. Cabid and L. Benguigui, J. Phys. France, 38, 961(1977).
14. D. W. Berreman, Mol. Cryst. Liq. Cryst., 22, 175(1973).
15. Y. Galerne and L. Liebert, Phys. Rev. Lett., 66, 906(1991).
16. A. D. L. Chandani, T. Hagiwara, Y.Suzuki, Y. Ouchi, H. Takezoe and A. Fukuda, Jpn J. Appl. Phys., 27, L729(1988).
17. A. D. L. Chandani, E. Gorecka, Y. Ouchi, H. Takezoe, and A. Fukuda, Jpn. J. Appl. Phys., 28, L1265(1989).